MDPI

Article

Linking Soil CO_2 Efflux to Individual Trees: Size-Dependent Variation and the Importance of the Birch Effect

Jonathan S. Schurman [1,2] and Sean C. Thomas [1,*]

1   Institute of Forestry and Conservation, University of Toronto, 33 Willcocks, Toronto, ON M5S 3B3, Canada; schurman@fld.czu.cz
2   Department of Forest Ecology, Faculty of Forestry and Wood Sciences, Czech University of Life Sciences, 165 00 Prague, Czech Republic
*   Correspondence: sc.thomas@utoronto.ca; Tel.: +1-416-978-1044

Abstract: Soil CO_2 efflux (F_{CO2}) is a major component of the terrestrial carbon (C) cycle but challenges in explaining local variability hamper efforts to link broad-scale fluxes to their biotic drivers. Trees are the dominant C source for forest soils, so linking tree properties to F_{CO2} could open new avenues to study plant-soil feedbacks and facilitate scaling; furthermore, F_{CO2} responds dynamically to meteorological conditions, complicating predictions of total F_{CO2} and forest C balance. We tested for proximity effects of individual *Acer saccharum* Marsh. trees on F_{CO2}, comparing F_{CO2} within 1 m of mature stems to background fluxes before and after an intense rainfall event. Wetting significantly increased background F_{CO2} (6.4 ± 0.3 vs. 8.6 ± 0.6 s.e. μmol CO_2 $m^{-2}s^{-1}$), with a much larger enhancement near tree stems (6.3 ± 0.3 vs. 10.8 ± 0.4 μmol CO_2 $m^{-2}s^{-1}$). F_{CO2} varied significantly among individual trees and post-rain values increased with tree diameter (with a slope of 0.058 μmol CO_2 $m^{-2}s^{-1}cm^{-1}$). Post-wetting amplification of F_{CO2} (the 'Birch effect') in root zones often results from the improved mobility of labile carbohydrates and further metabolization of recalcitrant organic matter, which may both occur at higher densities near larger trees. Our results indicate that plant-soil feedbacks change through tree ontogeny and provide evidence for a novel link between whole-system carbon fluxes and forest structure.

Keywords: Birch effect; carbon flux; ecosystem function; intraspecific variation; plant-soil interaction; soil respiration; tree ontogeny

1. Introduction

Soil carbon dioxide efflux (F_{CO2}) is the predominant contributor of CO_2 to the atmosphere from terrestrial ecosystems, with the balance between net photosynthesis and F_{CO2} largely determining whether a given ecosystem constitutes a net carbon (C) source or sink [1]. Recent decades have seen a shift in how F_{CO2} is conceptualized—from a flux largely reflecting ecosystem-specific decomposition and its response to soil temperature and moisture, to a process highly influenced by active and mutual exchanges between plants and soil biota [2]. Such feedbacks between plants and soil biota play a stabilizing role in numerous ecosystem functions and allow for plant regulation of biogeochemical cycles [3,4]; however, the specific role of biota is often neglected in studies of F_{CO2} conducted at higher levels of aggregation, because belowground sources are difficult to disentangle, and because abiotic signals, especially temperature, may be more clearly expressed on spatially integrated data [2]. As a result, the representation of plants and associated biota in ecosystem process models remains rather simplistic and temperature generally stands as the most common driving variable considered in ecosystem models of soil C processes [5–7]. However, without deeper insight into the biotic drivers of soil F_{CO2}, it will remain extremely challenging to link localized observations to broader scale, ecosystem-level fluxes and to develop process-driven predictions of future F_{CO2} dynamics [2,4].

Studies quantifying F_{CO2} in forest ecosystems commonly find high spatial variability that is not readily explained by edaphic or other environmental variables [8–10]. Spatial patchiness in F_{CO2} partially derives from the poor mobility of belowground C inputs through the soil matrix, with further temporal variability contributed by the responses of autotrophs and heterotrophs to short timescale (hourly to daily) meteorological variability [11,12]. A prominent phenomenon exemplifying the spatiotemporal complexity of localized F_{CO2} involves the dramatic spikes in F_{CO2} that follow rainfall events, also known as the 'Birch effect' [13,14]. The Birch effect is commonly attributed to the sudden mobilization of labile carbon inputs (e.g., energy-rich carbohydrates from litter and root exudates) by rainwater, which primes microbial assemblages, allowing further decomposition of lower-quality organic matter (e.g., from macroscopic necrotic tissues and humified organic matter) [14]. Increased osmoregulatory activity and rapid turnover of lysed microbes may also contribute to enhanced C fluxes [14]. Linking biotic sources of F_{CO2} to the broad-scale outputs of ecosystem models may therefore require attention to high temporal variability in meteorology and could further benefit from spatially explicit consideration of C inputs [15,16].

F_{CO2} depends directly on primary productivity, and, surprisingly, productivity effects can be even larger than temperature effects [17,18]. Tree girdling experiments and isotopic tracing measurements suggest that as much as 50% of CO_2 emitted from forest soils is sustained by recently produced photosynthates [19,20], implying that physiological changes occurring in tree canopies likely impact F_{CO2}. The ability to isolate the contribution of individual trees to F_{CO2} has further been demonstrated in a sparsely-treed savanna, where the diurnal pattern of F_{CO2} in individual tree root-zones was larger in amplitude than could be explained by temperature, and lagged the diurnal up-regulation of photosynthesis, corresponding to the transport time of sugars from foliage to roots [21]. Recognizing the potential to isolate tree-level F_{CO2} motivates further efforts to link such observations to traits governing the quantities of C exported from trees to external C sinks [4].

A number of recent studies have documented detectable local effects of tree proximity and even tree species on F_{CO2} [3,22–24], but the hypothetical mechanisms behind these effects are numerous and remain poorly resolved. Studies have also described effects of tree size on F_{CO2} in forest ecosystems, generally finding higher F_{CO2} in the immediate neighborhood of larger trees [25–30]. However, counterexamples exist [10,31], and several chrono sequence studies have found reduced F_{CO2} with stand age in even-aged plantations [32,33], or no consistent relationship [34]. Rodríguez-Calcerrada et al., [35] tested for associations between visible crown health indicators and F_{CO2} in an open woodland in Spain but found that increased plant recruitment near declining trees offset potential reductions in F_{CO2} related to tree decline. The character of C supply could theoretically shift as trees age from active extrusion of labile root exudates by more productive trees to less bioavailable necrotic tissues, but the connection between local tree effects on F_{CO2} and tree senescence or health status has received little attention.

Age-related trends in tree physiology are particularly large and well-documented in *Acer saccharum* Marsh. (hereafter sugar maple), a dominant tree in northern hardwood forests in Eastern North America. Leaf-level photosynthetic capacity peaks at intermediate sizes and declines later in ontogeny [36], and there is evidence for declines in whole-tree leaf area through ontogeny [37]. These trends are expected to constrain the amount of C available for belowground allocation, consistent with age-related declines in concentrations of non-structural carbohydrates in other sinks, such as wood [38]. As the capacity to replace fine roots declines with overall function, roots are more likely to be constructed to last longer, have increased C:N ratios, and be more resistant to decomposition [39]. If accumulation of high-C:N organic matter in tree root zones is an important chemical change that occurs through ontogeny, then the moisture-induced priming of microbial communities (Birch effect) may likewise vary through tree ontogeny. Additional processes associated with large old trees that may affect F_{CO2} include the potential for warmer soils beneath sparser canopies and increased maintenance respiration of older root tissue,

paralleling age-related trends in leaf respiration [40]. The magnitude of Birch-effect F_{CO_2} pulses could be more pronounced near large trees, but studies to date have not examined potential local tree size influences on Birch effect peaks in F_{CO_2}.

In the present study we collected spatially explicit F_{CO_2} data in a large mapped forest plot to address the following questions: (1) Does F_{CO_2} in the immediate vicinity of adult sugar maple stems differ from background soil flux? (2) Is there detectable tree-to-tree variation in root zone F_{CO_2}, and if so, is such variation dependent on tree diameter, growth rate, or health status? (3) How does F_{CO_2} in background vs. root-zone locations respond to soil conditions, in particular wetting following an intense rainfall event?

2. Materials and Methods

2.1. Study Site

The Haliburton Forest Dynamics Plot (HFDP), is located within Haliburton Forest and Wildlife Reserve Ltd., Ontario, Canada (44°55′ N, 78°45′ W), and belongs to the CTFS-ForestGEO global network of large-scale forest research plots [41]. HFDP encompasses several forest community types characteristic of the Great Lakes–St. Lawrence region. Total plot area is approximately 13.5 ha, of which approximately two thirds is occupied by a stand of shade-tolerant hardwoods. These interior, upland communities are dominated by sugar maple (*Acer saccharum* Marsh.), followed by American beech (*Fagus grandifolia* Ehrh.), and yellow birch (*Betula alleghaniensis* Britt.); the sub-canopy species striped maple (*Acer pensylvanicum* L.) is also abundant. Soils in the Haliburton region are shallow, predominantly sandy loams derived from till of the underlying granitic bedrock. Annual precipitation is approximately 1050 mm, with a mean annual temperature of 5 °C [42].

2.2. Data Collection

Flux collars consisted of 5-cm-long cross-sections of 10-cm diameter PVC plumbing, beveled with a power sander. The beveled edge of the collar was twisted into soil just enough to hold firmly (~1 cm); extra care was taken to ensure that collar insertion did not damage tree root tissues. If obstructions were encountered or a root was damaged, the collar was relocated within 20 cm of its initial location. Collars were always allowed to settle for at least 48 h before sampling.

Background sites were selected to ensure that locations were displaced at least two meters from any trees ≥10 cm diameter at breast height (dbh, measured using a diameter tape at 1.3 m height). Each background site consisted of a set of three collars, arrayed in a triangle with an approximate distance of one meter between collars. Background sites were distributed among 21 fixed points on a 57-m grid, with nine more randomly selected locations (Figure 1); a combination of uniform and random points was used to achieve broad coverage of spatial variation yet ensure that background estimates were not biased by unobserved factors with spatially regular distributions. The locations of background sampling locations were adjusted slightly upon collar installation to exclude local low points with a tendency to accumulate water and locations with shallow soils or exposed bedrock that prevented insertion of flux collars. Patches of understory vegetation may also contribute to soil F_{CO_2} [35], and so were also avoided.
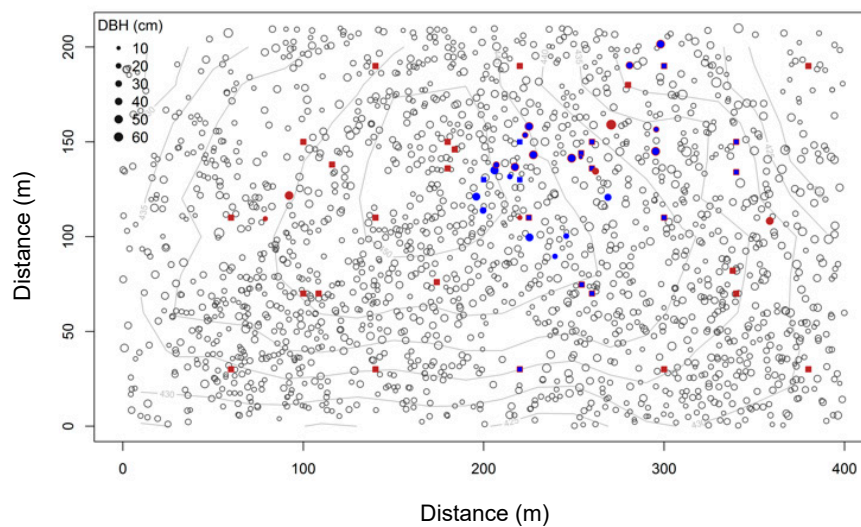
Figure 1. Map of adult sugar maple trees and soil efflux observations: all sugar maple stems with a diameter larger than 15 cm are indicated by empty circles. Bolded points indicate locations of soil efflux measurements. Squares are background fluxes; circles are tree-associated fluxes. Red symbols indicate pre-rain and blue symbols post-rain observations; blue symbols with a red outline indicate the locations with both pre- and post-rain observations. Topographic contours indicate 5-m elevation increments, ranging from 425 to 450 m.

Root zone F_{CO2} observations were collected from trees that were well spaced from neighboring individuals (minimum distance 3 m) on level terrain. Sampled focal trees varied from 10 to 55 cm dbh (corresponding to a crown radius of ~2 to 5 m). The majority of sampled trees were located on the interior plateau at the center of the forest plot, where composition is dominated by *Acer saccharum* and individual trees are well spaced (Figure 1). Canopy cover in the area is dense and spatially uniform and leaf-litter collection traps indicate that organic inputs in this section are also spatially uniform (data not shown). Measuring trees in the same neighborhood had the added advantage of minimizing underlying variation in soil drainage, texture, depth, and chemistry.

After study trees were selected, six soil efflux collars were inserted at a distance of approximately one meter from the base of each tree. Collars were distributed uniformly around each tree, except where obvious visible obstructions (vegetation, rocks, decayed logs) interfered. Several tree-level measurements were made to assess whether tree vitality influenced root-zone F_{CO2}. Tree dbh was recorded at the time of F_{CO2} sampling using a diameter tape and compared to a former census measurement collected in the year 2011 to estimate mean annual growth increment over the two-year period (radial increment in cm/y). Crown transparency measurements from a maple health survey conducted in July 2009 with moosehorn densiometers [43] were also used as a health status indicator for sampled trees.

2.3. Pre- and Post-Rain Sampling Intervals

The first round of sampling was done from 17–19 August 2013, with a subset of ten background and two root zone locations resampled on August 24th. A 42.2-mm rain event occurred on August 25th (Figure 2, Historical Climate Data, Environment Canada, Government of Canada) followed by a second round of sampling between August 27th and 29th. We were additionally able to validate the correspondence between temperature data with regional weather station and local temperatures at the soil surface with a network of 46 temperature loggers (Logtag, Auckland, New Zealand), which recorded soil temperatures just below the organic layer, spaced on a 28-m square grid throughout the study site. Mean daily soil surface temperatures and mean daily air temperatures from the regional station day were highly correlated (r = 0.94, data not shown).
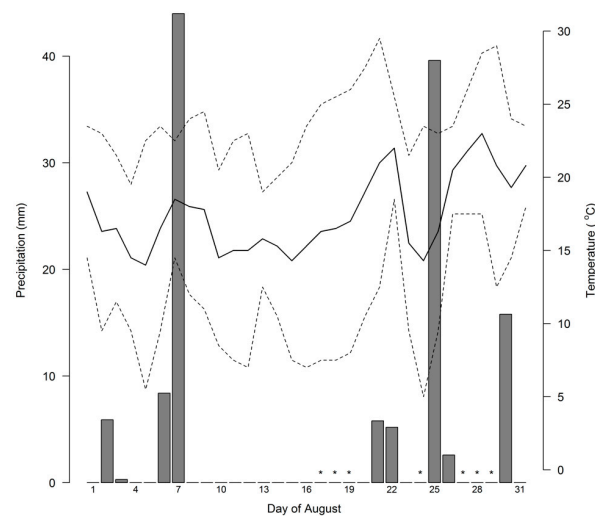
Figure 2. Haliburton regional weather data for August 2013. Lines indicate daily range (dashed) and mean (solid) temperatures. Bars indicate magnitude of rainfall. Points marked with asterisks along the x-axis indicate dates of flux observations.

2.4. Data Processing and Quality Control

In total, 30 background and 18 root zone fluxes were sampled before wetting and 14 background and 22 root zones after wetting. Soil CO_2 efflux (F_{CO2}) observations were made with a portable infrared gas analyzer (IRGA) with soil chamber attachment (Li6400 with Li-6400-09 attachment, LiCor, Lincoln, Nebraska). Mean temperature of the top 10 cm of soil was also recorded with a Li-6400-09TC thermocouple probe. The IRGA cuvette was sealed to the collar and approximately 30 to 60 s were allowed for CO_2 readings to stabilize before measurements. At least three F_{CO2} readings were logged, spaced at 30-s intervals, which were averaged prior to analysis. If collars demonstrated extreme values (greater than two standard deviations from the mean, or >50 μmol m^{-2} s^{-1}), the collar was removed and data from this location were not integrated into the analysis (this was done for 4 out of 278 collars).

2.5. Data Analysis

A two-way analysis of variance (ANOVA) was conducted to compare F_{CO2} of background to root zone locations, before and after rainfall. Where duplicate observations were available, the average of the two dates was used. For root zone F_{CO2} values associated with tree stems, each tree's F_{CO2} was calculated by averaging over its associated collars prior to analysis.

Increases in soil temperature characteristically result in multiplicative increases in F_{CO2}. To correct for temperature effects we modeled the temperature response of F_{CO2} using an exponential equation ($F_{CO2} = a*exp[b * T_{soil}]$), where T_{soil} = mean soil temperature to 10-cm depth, a and b are fitted parameters) to the full dataset of soil collars. Q_{10} provides a concise indicator of the temperature sensitivity of a F_{CO2} temperature responses curve and was estimated to allow for comparison among similar temperature responses analyses ($Q_{10} = exp[b * 10]$). A t-test was conducted to compare soil temperatures during pre-rain sampling and post-rain sampling.

The statistical residuals from the exponential model temperature response model provided temperature-corrected F_{CO2} indices, which were then compared to tree-level characteristics. To assess among-tree variation in root zone F_{CO2}, an additional one-way ANOVA with tree as a factor was performed, using temperature-corrected F_{CO2} values for pre- and post-precipitation root zone fluxes. Simple linear regressions were conducted to determine whether tree size, recent growth, or crown transparency were statistical predictors of root zone respiration. All analyses were performed in the 'stats' package of the R statistical programming language [44].

3. Results

3.1. Pre- vs. Post-Precipitation F_{CO2}

Soil CO_2 efflux preceding the rainfall event averaged 6.43 ($\pm$0.31 s.e.) μmol CO_2 m^{-2} s^{-1} and 6.25 ($\pm$0.29 s.e.) μmol CO_2 m^{-2} s^{-1} for background and root zones, respectively, which were not statistically distinguishable. Following the August 25th rainfall event, F_{CO2} significantly increased to 8.61 ($\pm$0.64 s.e.) μmol CO_2 m^{-2} s^{-1} and 10.79 ($\pm$0.41 s.e.) μmol CO_2 m^{-2} s^{-1} for background and root zone fluxes ($p_{wet} < 0.001$), respectively. A significant root zone by pre-/post-rainfall interaction term was also detected ($p_{RZ*Wet} = 0.005$), indicating that root zones fluxes experienced a larger enhancement following the rainfall event relative to background conditions (Figure 3).
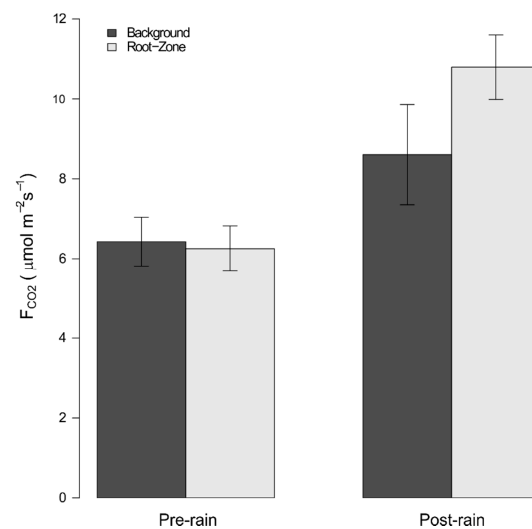

Figure 3. Response of background and root zone soil CO_2 flux to wetting. Error bars indicate 95% confidence intervals.

3.2. Temperature Effects on F_{CO2}

In addition to increased soil moisture, soil temperatures were also higher during post-rain sampling (14.8 ($\pm$0.09 s.e.) °C vs. 16.8 ($\pm$0.09 s.e.) °C; Figure 4a). We detected a statistically significant influence of temperature on F_{CO2} and this relationship was accurately captured with an exponential model ($F_{CO2} = 0.6189 \times e^{0.1651 \cdot Tsoil}$; $p < 0.001$) (Figure 4b), From this relationship, we further estimated a Q_{10} value of 5.81 ($\pm$0.45 s.e.).
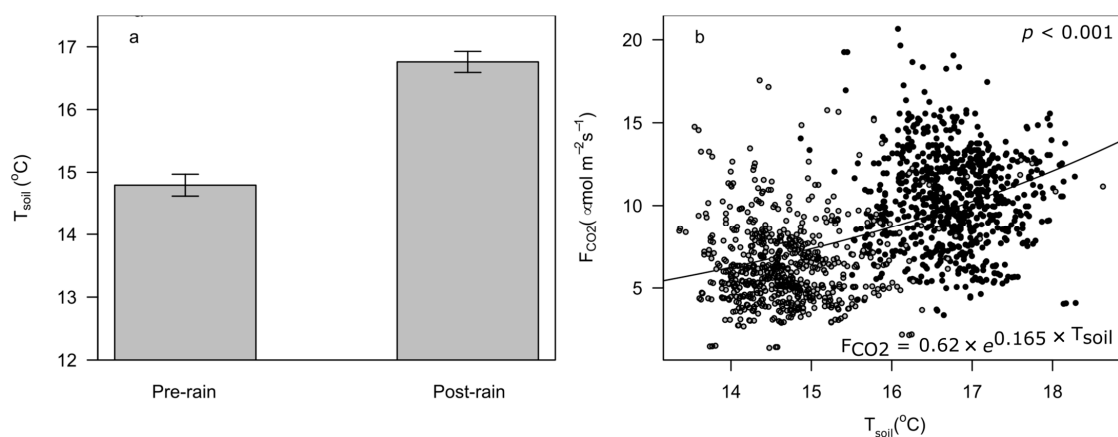

Figure 4. Soil temperature patterns and effects on soil CO_2 efflux. Soil temperatures (T_{soil}) before and after wetting were significantly different ((**a**), $p < 0.001$, error bars indicate 95% confidence intervals). Observed fluxes were sensitive to soil temperatures (**b**). The exponential rate of increase was estimated to be $Q_{10} = 5.81$ ($\pm$ 0.45 s.e.). Open dots indicate pre-rain soil fluxes observations and filled dots indicate post-rain fluxes.

3.3. Tree Effects on F_{CO2}

Post-rain temperature-corrected root zone F_{CO2} was positively related to tree dbh (Figure 5b). Following rain, root-zone F_{CO2} increased at a rate of 0.058 µmol m^{-2} s^{-1} for every centimeter increase in tree dbh ($p = 0.040$, $r^2 = 0.154$). We did not detect a significant effect of tree size on pre-rain F_{CO2} (Figure 5a). The other metrics examined, radial increment and crown transparency, were not able to explain any variation in temperature corrected effluxes among trees either pre- or post-rain. Although tree size appeared to be the only metric to influence F_{CO2}, ANOVA results showed statistically significant variation among individuals in temperature-corrected efflux, both before and after the rainfall event ($p < 0.001$ for both ANOVAs) (Figure 5), indicating additional among-tree variation.
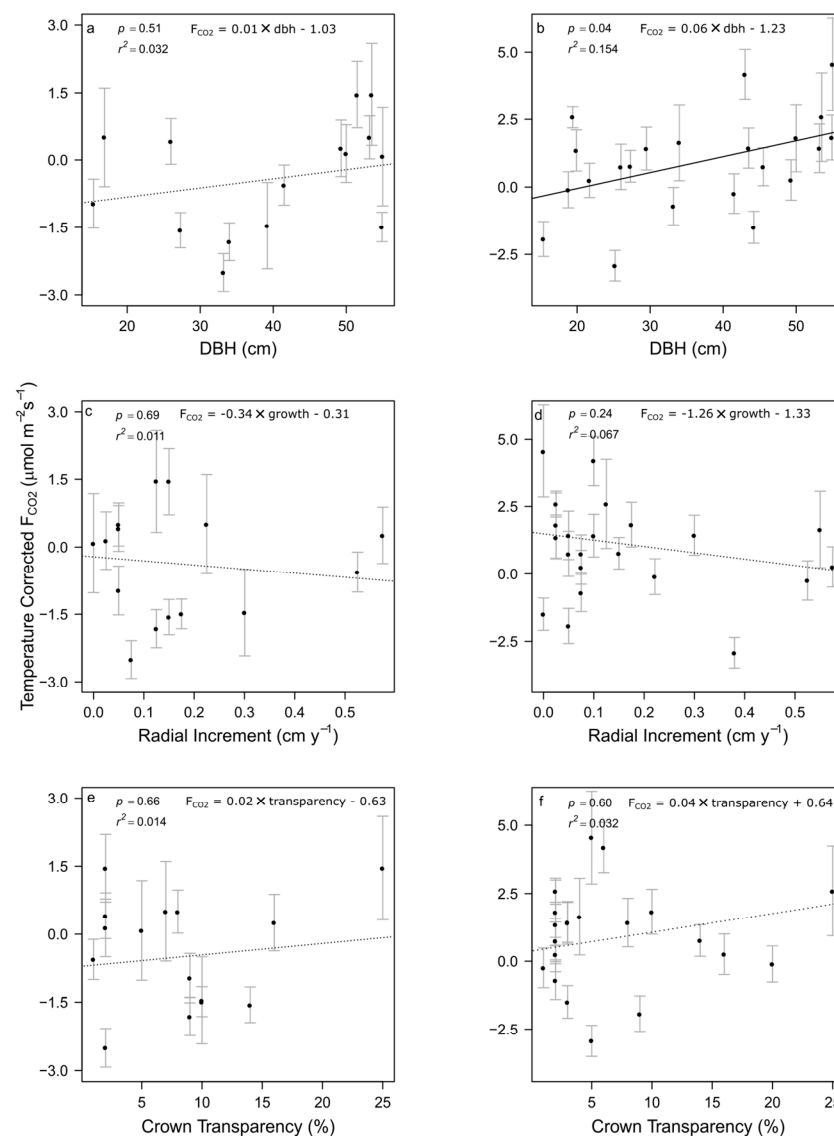

Figure 5. Relationships between individual tree characteristics and temperature-corrected soil CO_2 efflux. Error bars represent standard error (n = 6) in each individual tree's root zone flux. Significant variation was detected among individual tree root zones both before (panels (**a,c,e**)) and after (panels (**b,d,f**)) wetting (p_{dry} and $p_{wet} < 0.001$). Post-rain variation in soil root zone fluxes was significantly related to tree dbh (solid regression line) but not to other variables (dotted regression lines).

4. Discussion

Our objective was to determine whether the contribution of individual trees to soil F_{CO2} could be detected by comparing root zone F_{CO2} to background variation, and to

further link aboveground properties of *A. saccharum* trees to belowground C processes in a closed-canopy forest. Under typical conditions, root-zone F_{CO2} did not differ from background F_{CO2} but was significantly higher following an intense precipitation event. We also detected significant variation among individual root-zone F_{CO2} estimates, both before and after rainfall. Temperature-corrected F_{CO2} increased significantly with tree size, consistent with prior studies [25–30]; however, this pattern was only detected for post-precipitation F_{CO2}. We did not find any trend with tree health indicators (either recent tree growth increment or crown transparency), suggesting that the size-dependent pattern in F_{CO2} is not related to tree senescence.

Transient 'Birch effect' increases in F_{CO2} in response to wetting is a well-documented phenomenon [13,14]. Elevated F_{CO2} typically persists for several days after moisture increases and is mainly attributed to the improved mobilization of labile carbon compounds, which primes microbial communities for further degradation of less bioavailable substrates [14]. Root exclusion studies have also found that the Birch effect depends on root presence [45]. Our results indicate that the Birch effect is both more pronounced in the vicinity of tree stems and is greater in magnitude near larger trees. Prior studies examining tree-size effects on F_{CO2} have not explicitly tested for Birch-effect patterns, but Søe and Buchmann [26] found that a best-fitting model describing variation in F_{CO2} included both tree size (mean dbh of trees within 4 m radius), and volumetric soil moisture content; Schwendenmann and Macinnis-Ng [30] noted relatively dry soil conditions near the base of large trees that could enhance the gas diffusion, and so increase F_{CO2}.

Several mechanisms might contribute to the tree-size-dependent Birch effect detected in the present study. Mobility of labile C substrates, such as root exudates, is limited by diffusion, and these labile C compounds could thus accumulate in the immediate vicinity of their source [46]. Larger trees with larger canopies are generally more productive and may export larger quantities of carbohydrates to associated soil biota, which accumulate until rain-induced mobilization. It is furthermore likely that necrotic tissues such as dead fine roots, which are an important carbon source for heterotrophic respiration [47], occur at higher densities in the root zones of larger trees. These higher-density pools of low-quality organic matter are more accessible to microbial communities following wetting events. An additional possibility consists of a more biophysical mechanism, where larger canopy areas may intercept larger quantities of moisture, leading to higher stemflow and higher moisture near the bases of large trees [48].

Among-tree variation in root zone F_{CO2} was not significantly correlated with tree size prior to rainfall, but we did detect significant variation among individuals. This additional variation among locations could be explained by topography and unobserved edaphic variables, but also invites deeper explorations of how tree health status could also regulate soil F_{CO2}. For example, Hancock et al. [49] found that the early stages of infection of *Fagus grandifolia* by the invasive pathogen *Neonectria* (beech-bark disease) corresponded with sharply increased local F_{CO2}. Geddes et al. [50] reported anomalous ecosystem-level C losses from a stand co-dominated by *Fagus grandifolia* at HFWR and considered the onset of beech-bark disease a likely explanation. We speculate that pathogen infection may more generally contribute to high tree-to-tree variation in F_{CO2} and component processes.

Although biotic factors have been found to dominate soil F_{CO2} in studies conducted at comparable scales to the present analysis [17,18], we still found that correcting for temperature effects was essential for detecting tree size effects on soil F_{CO2}. Soil temperatures were clearly sensitive to changes in ambient air temperature over the duration of the study, with impacts on F_{CO2} (Figure 3). However, the estimated sensitivity of F_{CO2} to temperature in the present study was substantially higher than estimates from comparable forest soils (compare our estimated Q_{10} of 5.8, to a prior estimate of 3.0 at HFWR [8], and 3.5 at a comparable site in New England [51]). This high sensitivity is almost certainly due to coupled increases in soil moisture and temperature, which likely had a compound effect on soil F_{CO2}. This observation further highlights the need to sample over wider ranges of variation in meteorological conditions, whereas studies of plant-soil systems often aim to

narrow the range of environmental variation in an effort to improve their ability to detect specific biotic interactions.

The ability to anticipate ecosystem-level responses of soil respiration to the changing climate is still limited by our understanding of relationships between soil moisture and microbial respiration [16]. The Birch effect is frequently left out of ecosystem-level models of C exchange entirely [16], even though this has been shown to result in a ~25% underestimation of soil C emissions, at least in northern deciduous forests [52]. Changes in the isotopic composition of C emissions over very short periods following moisture pulses indicate that inorganic C can also contribute to the Birch effect in some systems [53]. Uncertainty in these sources of C emissions limits the applicability of otherwise analytically tractable process-based models that incorporate the kinetics of C supply and microbe consumption [54]. Our results suggest that Birch effect fluxes may be specifically enhanced in forests with large, old trees, potentially indicating an underestimation of carbon losses from old-growth forests without explicit consideration.

5. Conclusions

The present study compliments prior work suggesting strong autotrophic control over F_{CO2}. Our work replicates prior studies indicating a size-dependent increase in F_{CO2}, while also demonstrating a strong ontogenetic trend in carbon flux associated with the Birch effect. Detecting tree size effects on soil CO_2 efflux invites the investigation of additional biophysical and biogeochemical relations that may be impacted by the ontogeny and/or allometry of tree root functioning and organic matter production. Unifying physiological mechanisms with ecosystem modeling efforts requires replication of comparable measurements across tree species and over a wider range of environmental variation, including rainfall intensity, rainfall frequency, and seasonal variation in belowground photosynthate allocation.

References

1. Schlesinger, W.H.; Andrews, J.A. Soil respiration and the global carbon cycle. *Biogeochemistry* **2000**, *481*, 7–20. [CrossRef]
2. van der Putten, W.H.; Bardgett, R.D.; Bever, J.D.; Bezemer, T.M.; Casper, B.B.; Fukami, T.; Kardol, P.; Klironomos, J.N.; Kulmatiski, A.; Schweitzer, J.A.; et al. Plant-soil feedbacks: The past, the present and future challenges. *J. Ecol.* **2013**, *101*, 265–276. [CrossRef]
3. van Haren, J.; de Oliveira, R.C., Jr.; Beldini, P.T.; de Camargo, P.B.; Keller, M.; Saleska, S. Tree species effects on soil properties and greenhouse gas fluxes in East-Central Amazonia: Comparison between monoculture and diverse forest. *Biotropica* **2013**, *456*, 709–718. [CrossRef]
4. Chapin, F.S., III; McFarland, J.; McGuire, A.D.; Euskirchen, E.S.; Ruess, R.W.; Kielland, K. The changing global carbon cycle: Linking plant-soil carbon dynamics to global consequences. *J. Ecol.* **2009**, *97*, 840–850.
5. Friedlingstein, P.; Cox, P.; Betts, R.; Bopp, L.; Von Bloh, W.; Brovkin, V.; Cadule, P.; Doney, S.; Eby, M.; Fung, I.; et al. Climate–carbon cycle feedback analysis: Results from the C 4 MIP model intercomparison. *J. Clim.* **2006**, *19*, 3337–3353. [CrossRef]

6. Kirschbaum, M.U.F. The temperature dependence of organic-matter decomposition—still a topic of debate. *Soil Biol. Biochem.* **2006**, *38*, 2510–2518. [CrossRef]
7. Subke, J.A.; Bahn, M. On the "temperature sensitivity" of soil respiration: Can we use the immeasurable to predict the unknown? *Soil Biol. Biochem.* **2010**, *42*, 1653–1656. [CrossRef] [PubMed]
8. Peng, Y.; Thomas, S.C. Soil CO_2 efflux in uneven-aged managed forests: Temporal patterns following harvest and effects of edaphic heterogeneity. *Plant Soil* **2006**, *289*, 253–264. [CrossRef]
9. Knohl, A.; Søe, A.R.; Kutsch, W.L.; Göckede, M.; Buchmann, N. Representative estimates of soil and ecosystem respiration in an old beech forest. *Plant Soil* **2008**, *302*, 189–202. [CrossRef]
10. Ngao, J.; Epron, D.; Delpierre, N.; Bréda, N.; Granier, A.; Longdoz, B. Spatial variability of soil CO_2 efflux linked to soil parameters and ecosystem characteristics in a temperate beech forest. *Agric. For. Meteorol.* **2012**, *154*, 136–146. [CrossRef]
11. Bardgett, R.D.; Bowman, W.D.; Kaufmann, R.; Schmidt, S.K. A temporal approach to linking aboveground and belowground ecology. *Trends Ecol. Evol.* **2005**, *20*, 634–641. [CrossRef] [PubMed]
12. Högberg, P.; Read, D.J. Towards a more plant physiological perspective on soil ecology. *Trends Ecol. Evol.* **2006**, *21*, 548–554. [CrossRef] [PubMed]
13. Birch, H.F. The effect of soil drying on humus decomposition and nitrogen availability. *Plant Soil* **1958**, *10*, 9–31. [CrossRef]
14. Borken, W.; Matzner, E. Reappraisal of drying and wetting effects on C and N mineralization and fluxes in soils. *Glob. Chang. Biol.* **2009**, *15*, 808–824. [CrossRef]
15. Vargas, R.; Carbone, M.S.; Reichstein, M.; Baldocchi, D.D. Frontiers and challenges in soil respiration research: From measurements to model-data integration. *Biogeochemistry* **2011**, *102*, 1–13. [CrossRef]
16. Vicca, S.; Bahn, M.; Estiarte, M.; van Loon, E.E.; Vargas, R.; Alberti, G.; Ambus, P.; Arain, M.A.; Beier, C.; Bentley, L.P.; et al. Can current moisture responses predict soil CO_2 efflux under altered precipitation regimes? A synthesis of manipulation experiments. *Biogeosciences* **2014**, *11*, 853–899.
17. Janssens, I.A.; Lankreijer, H.; Matteucci, G.; Kowalski, A.S.; Buchmann, N.; Epron, D.; Pilegaard, K.; Kutsch, W.; Longdoz, B.; Grünwald, T.; et al. Productivity overshadows temperature in determining soil and ecosystem respiration across European forests. *Glob. Chang. Biol.* **2001**, *7*, 269–278. [CrossRef]
18. Bahn, M.; Rodeghiero, M.; Anderson-Dunn, M.; Dore, S.; Gimeno, C.; Drösler, M.; Williams, M.; Ammann, C.; Berninger, F.; Flechard, C.; et al. Soil respiration in European grasslands in relation to climate and assimilate supply. *Ecosystems* **2008**, *11*, 1352–1367. [CrossRef]
19. Högberg, P.; Nordgren, A.; Buchmann, N.; Taylor, A.F.S.; Ekblad, A.; Högberg, M.N.; Nyberg, G.; Ottosson-Löfvenius, M.; Read, D.J. Large-scale forest girdling shows that current photosynthesis drives soil respiration. *Nature* **2001**, *411*, 789–792.
20. Högberg, P.; Högberg, M.N.; Göttlicher, S.G.; Betson, N.R.; Keel, S.G.; Metcalfe, D.B.; Campbell, C.; Schindlbacher, A.; Hurry, V.; Lundmark, T.; et al. High temporal resolution tracing of photosynthate carbon from the tree canopy to forest soil microorganisms. *New Phytol.* **2008**, *177*, 220–228. [CrossRef]
21. Tang, J.; Baldocchi, D.D. Spatial-temporal variation in soil respiration in an oak-grass savanna ecosystem in California and its partitioning into autotrophic and heterotrophic components. *Biogeochemistry* **2005**, *73*, 183–207. [CrossRef]
22. Bréchet, L.; Ponton, S.; Roy, J.; Freycon, V.; Coûteaux, M.M.; Bonal, D.; Epron, D. Do tree species characteristics influence soil respiration in tropical forests? A test based on 16 tree species planted in monospecific plots. *Plant Soil* **2009**, *319*, 235–246. [CrossRef]
23. Vesterdal, L.; Elberling, B.; Christiansen, J.R.; Callesen, I.; Schmidt, I.K. Soil respiration and rates of soil carbon turnover differ among six common European tree species. *For. Ecol. Manag.* **2009**, *264*, 185–196. [CrossRef]
24. Li, W.; Bai, Z.; Jin, C.; Zhang, X.; Guan, D.; Wang, A.; Yuan, F.; Wu, J. The influence of tree species on small scale spatial heterogeneity of soil respiration in a temperate mixed forest. *Sci. Total Environ.* **2017**, *590*, 242–248. [CrossRef] [PubMed]
25. Bréchet, L.; Ponton, S.; Alméras, T.; Bonal, D.; Epron, D. Does spatial distribution of tree size account for spatial variation in soil respiration in a tropical forest? *Plant Soil* **2011**, *347*, 293. [CrossRef]
26. Søe, A.R.; Buchmann, N. Spatial and temporal variations in soil respiration in relation to stand structure and soil parameters in an unmanaged beech forest. *Tree Physiol.* **2005**, *2511*, 1427–1436. [CrossRef]
27. Katayama, A.; Kume, T.; Komatsu, H.; Ohashi, M.; Nakagawa, M.; Yamashita, M.; Otsuki, K.; Suzuki, M.; Kumagai, T. Effect of forest structure on the spatial variation in soil respiration in a Bornean tropical rainforest. *Agric. For. Meteorol.* **2009**, *149*, 1666–1673. [CrossRef]
28. Luan, J.; Liu, S.; Zhu, X.; Wang, J.; Liu, K. Roles of biotic and abiotic variables in determining spatial variation of soil respiration in secondary oak and planted pine forests. *Soil Biol. Biochem.* **2012**, *441*, 143–150. [CrossRef]
29. ArchMiller, A.A.; Samuelson, L.J.; Li, Y. Spatial variability of soil respiration in a 64-year-old longleaf pine forest. *Plant Soil* **2016**, *403*, 419–435. [CrossRef]
30. Schwendenmann, L.; Macinnis-Ng, C. Soil CO_2 efflux in an old-growth southern conifer forest *Agathis australis*—magnitude, components and controls. *Soil* **2016**, *23*, 403–419. [CrossRef]
31. Song, Q.H.; Tan, Z.H.; Zhang, Y.P.; Cao, M.; Sha, L.Q.; Tang, Y.; Liang, N.S.; Schaefer, D.; Zhao, J.F.; Zhao, J.B.; et al. Spatial heterogeneity of soil respiration in a seasonal rainforest with complex terrain. *iForest-Biogeosci. For.* **2013**, *62*, 65–72. [CrossRef]
32. Ryan, M.G.; Yoder, B.J. Hydraulic limits to tree height and tree growth. *Bioscience* **1997**, *47*, 235–242. [CrossRef]

33. Saiz, G.; Green, C.; Butterbach-Bahl, K.; Kiese, R.; Avitabile, V.; Farrell, E.P. Seasonal and spatial variability of soil respiration in four Sitka spruce stands. *Plant Soil* **2006**, *287*, 161–176. [CrossRef]

34. Powers, M.; Kolka, R.; Bradford, J.; Palik, B.; Jurgensen, M. Forest floor and mineral soil respiration rates in a northern Minnesota red pine chrono sequence. *Forests* **2018**, *9*, 16. [CrossRef]

35. Rodríguez-Calcerrada, J.; Salomón, R.; Barba, J.; Gordaliza, G.G.; Curiel Yuste, J.; Magro, C.; Gil, L. Regeneration in the understory of declining overstory trees contributes to soil respiration homeostasis along succession in a sub-Mediterranean beech forest. *Forests* **2019**, *10*, 727. [CrossRef]

36. Thomas, S.C. Photosynthetic capacity peaks at intermediate size in temperate deciduous trees. *Tree Physiol.* **2010**, *30*, 555–573. [CrossRef]

37. Nock, C.A.; Caspersen, J.P.; Thomas, S.C. Large ontogenetic declines in intra-crown leaf area index in two temperate deciduous tree species. *Ecology* **2008**, *89*, 744–753. [CrossRef]

38. Martin, A.R.; Thomas, S.C. Size-dependent changes in leaf and wood chemical traits in two Caribbean rainforest trees. *Tree Physiol.* **2013**, *33*, 1338–1353. [CrossRef]

39. Eissenstat, D.M.; Yanai, R.D. The ecology of root lifespan. *Adv. Ecol. Res.* **1997**, *27*, 1–60.

40. Thomas, S.C.; Winner, W.E. Photosynthetic differences between saplings and adult trees: An integration of field results by meta-analysis. *Tree Physiol.* **2002**, *22*, 117–127. [CrossRef]

41. Anderson-Teixeira, K.J.; Davies, S.J.; Bennett, A.C.; Gonzalez-Akre, E.B.; Muller-Landau, H.C.; Wright, S.J.; Salim, K.A.; Zambrano, A.M.A.; Alonso, A.; Baltzer, J.L.; et al. CTFS-ForestGEO: A worldwide network monitoring forests in an era of global change. *Global Change Biol.* **2014**, *21*, 528–549. [CrossRef] [PubMed]

42. Environment Canada, Government of Canada, Historical Climate Data, Haliburton Ontraio. Available online: http://climate.weather.gc.ca/ (accessed on 9 November 2014).

43. Garrison, G.A. Uses and modifications for the "moosehorn" crown closure estimator. *J. For.* **1949**, *47*, 733–735.

44. R Core Team. *R: A Language and Environment for Statistical Computing*; R Foundation for Statistical Computing: Vienna, Austria, 2013.

45. Tang, J.; Misson, L.; Gershenson, A.; Cheng, W.; Goldstein, A.H. Continuous measurements of soil respiration with and without roots in a ponderosa pine plantation in the Sierra Nevada Mountains. *Agric. For. Meteorol.* **2005**, *132*, 212–227. [CrossRef]

46. Jones, D.L.; Hodge, A.; Kuzyakov, Y. Plant and mycorrhizal regulation of rhizodeposition. *New Phytol.* **2004**, *163*, 459–480. [CrossRef]

47. Gill, R.A.; Jackson, R.B. Global patterns of root turnover for terrestrial ecosystems. *New Phytol.* **2000**, *147*, 13–31. [CrossRef]

48. Levia, D.F.; Keim, R.F.; Carlyle-Moses, D.E.; Frost, E.E. Throughfall and stemflow in wooded ecosystems. In *Forest Hydrology and Biogeochemistry*; Levia, D.F., Carlyle-Moses, D., Tanaka, T., Eds.; Springer: Dordrecht, The Netherlands, 2011; pp. 425–443.

49. Hancock, J.E.; Arthur, M.A.; Weathers, K.C.; Lovett, G.M. Carbon cycling along a gradient of beech bark disease impact in the Catskill Mountains, New York. *Can. J. For. Res.* **2008**, *385*, 1267–1274. [CrossRef]

50. Geddes, J.A.; Murphy, J.G.; Schurman, J.S.; Petroff, A.; Thomas, S.C. Net ecosystem exchange of an uneven-aged managed forest in central Ontario, and the impact of a spring heat wave event. *Agric. For. Meteorol.* **2014**, *198*, 105–115. [CrossRef]

51. Boone, R.D.; Nadelhoffer, K.J.; Canary, J.D.; Kaye, J.P. Roots exert a strong influence on the temperature sensitivity of soil respiration. *Nature* **1998**, *396*, 570–572. [CrossRef]

52. Lee, X.; Wu, H.J.; Sigler, J.; Oishi, C.; Siccama, T. Rapid and transient response of soil respiration to rain. *Glob. Chang. Biol.* **2004**, *106*, 1017–1026. [CrossRef]

53. Inglima, I.; Alberti, G.; Bertolini, T.; Vaccari, F.P.; Giolo, B.; Miglietta, F.; Cotrufo, M.F.; Peressotti, A. Precipitation pulses enhance respiration of Mediterranean ecosystems: The balance between organic and inorganic components of increased soil CO_2 efflux. *Glob. Chang. Biol.* **2009**, *155*, 1289–1301. [CrossRef]

54. Moyana, F.E.; Manzoni, S.; Chenu, C. Responses of soil heterotrophic respiration to moisture availability: An exploration of processes and models. *Soil Biol. Biochem.* **2013**, *59*, 72–85. [CrossRef]